Phase relations among smectite, R1 illite-smectite, and illite

HAILIANG DONG,[1] DONALD R. PEACOR,[1] AND ROBERT L. FREED[2]

[1]Department of Geological Sciences, University of Michigan, Ann Arbor, Michigan 48109-1063, U.S.A.
[2]Department of Geology, Trinity University, San Antonio, Texas 78212, U.S.A.

ABSTRACT

A variety of smectitic and illitic clays were studied by TEM and AEM, following expansion by L.R. White resin, to define phase relations for clay minerals undergoing digenesis and low-grade metamorphism. Samples included a prograde shale sequence from the Gulf Coast, a hydrothermal bentonite from Zempleni, Hungary, and shales from the Nankai Trough, Japan, Michigan, and the Welsh sedimentary basin. All samples were dominated by various proportions of only three kinds of clay minerals: smectite having no 10 Å layers, R1 illite-smectite (I/S) (50% illite), and illite with only small proportions of smectite-like interlayers; mixed-layer phases with intermediate ratios of I/S were observed only as minor components of other layer sequences. Lattice fringe images show that the common layer spacing of R1 I/S is 21 Å and that it has 0.7–0.8 K pfu; its properties are not an average of those of smectite and illite, which is consistent with the uniqueness of the R1 I/S structure.

A prograde sequence of clay mineral transitions in the studied samples can be characterized by five stages with different combinations of the three major phases (i.e., smectite, R1 I/S, and illite) corresponding to different grades. The sequence from low to high grade is (1) pure smectite, (2) smectite with small proportions of discrete R1 I/S and illite, (3) R1 I/S with small proportions of smectite and illite, (4) illite with some R1 I/S and smectite, and (5) illite. Common exceptions to this scheme are inferred to be caused by the inherent metastability of all phases, in occurrences that are rate or path dependent.

INTRODUCTION

It is generally accepted among clay mineralogists, in part from the influence of the classic paper of Hower et al. (1976), that the sedimentary smectite-to-illite transition occurs through a sequence of illite-smectite phases (commonly denoted I/S), including smectite-rich R0 I/S, R1 I/S, R2 I/S, and R3 I/S, and illite-rich I/S, with continuously variable ratio in the proportions of smectite- and illite-like layers. According to this model, the relative proportion of illite interlayers increases until no expandable layers remain, during progressive prograde digenesis and low-grade metamorphism of pelitic rocks. This model implies that all I/S with relative numbers of illite layers from 0 to 100% are likely to occur. This concept led in part to the implication inherent in the work of Hower et al. (1976) that the smectite-to-illite transition could proceed layer by layer, i.e., individual smectite layers may be progressively replaced by illite layers with loss of Si, Na, and H_2O and gain of K and Al during the transformation process.

However, several recent TEM studies indicate that R1 I/S with 50% I is relatively abundant, whereas other kinds of mixed-layer I/S phases (e.g., R0 I/S, R1 I/S with > 50% I, R3 I/S, etc.) are rarely observed (Ahn and Peacor 1989; Veblen et al. 1990; Jiang et al. 1990a; Dong and Peacor 1996; Sears, personal communication). Ahn and

Peacor (1989) observed only R1 I/S, but not R2 or R3 I/S, in a Gulf Coast sample (5500 m depth), using the overfocus conditions recommended by Guthrie and Veblen (1989a, 1989b, 1990). The presence of R1 I/S at the 5500 m depth is consistent with XRD data on the same sample (Ahn and Peacor 1989). They further concluded that caution should be exercised in estimating the relative proportion of R1 I/S based on TEM images only, because even though ordering exists over the whole image, it may be observed in rather limited areas with great difficulty, largely because of variable orientations of layers relative to the electron beam. This conclusion implies that R1 I/S observed in TEM images represents a minimum of that actually present in original rocks.

Ahn and Peacor (1986) proposed a dissolution-precipitation model for the smectite-to-illite transformation. This model suggests that a reactant, smectite, is structurally disarticulated and individual chemical components are transported through fluid and reorganized and precipitated as a new phase. Jiang et al. (1990a) noted that the chemical composition of R1 I/S is not a weighted average of those for smectite and illite, indicating that R1 I/S is a unique phase. The observation by Jiang et al. (1990a) is consistent with neoformation of all layers, i.e., even the 2:1 structure units associated with expandable interlayers must have compositions richer in Al and poorer in

Si than original smectite, which is feasible only with disarticulation of all original smectite 2:1 layers. These relations suggest that all portions of crystals are affected by dissolution-precipitation.

Among trioctahedral phyllosilicates, there is a sequence from Mg-rich smectite (saponite) to corrensite to chlorite, which is analogous to that among dioctahedral phyllosilicates. Corrensite has an ordered 1:1 structure (Roberson et al. 1996) analogous to that of 1:1 R1 I/S (rectorite). Shau et al. (1990b) and Reynolds (1988) have inferred that corrensite is a unique phase in terms of its composition and structure, i.e., it does not consist merely of equal numbers of ordered smectite and chlorite interlayers, each of which is effectively identical to layers in the pure end-members. The hydrothermal synthesis experiments by Roberson et al. (1996) verified that corrensite is chemically and structurally unique. It is well established that corrensite is the only ordered mixed-layer phase among the Mg-rich smectite-chlorite series, that it commonly coexists with either saponite or chlorite, and that it is abundant relative to mixed layer chlorite-smectite (C/S) with any other ratio of layers, which is consistent with minimum free energy and a characteristic, unique structure.

A more familiar example of the uniqueness of ordered, mixed-layered structures is in the system $CaCO_3$-$MgCO_3$, where dolomite can be viewed as 1:1 ordered, mixed-layer $CaCO_3$-$MgCO_3$. The analogy between R1 I/S and dolomite is not rigorous, however, because R1 I/S does not have a composition corresponding to 50% smectite and 50% illite (Jiang et al. 1990a), whereas dolomite does have a composition corresponding to 50% calcite and 50% magnesite. In addition, the structure of R1 I/S is poorly known. Nevertheless, the calcite-magnesite system is analogous to the smectite-illite system in terms of the 1:1 ordering scheme. The interaction between layers of the dolomite structure leads to distortions in Ca and Mg coordination polyhedra that cause the structure to be unique in detail relative to those of calcite and magnesite (Reeder 1983). This in turn leads to relative thermodynamic stability of dolomite, which is analogous with that for R1 I/S, and co-occurrence of calcite + dolomite and dolomite + magnesite, rather than a continuum of mixed-layer phases with intermediate ratios of $CaCO_3$ and $MgCO_3$.

Although the detailed crystal structures of smectite and I/S have not been determined, indirect evidence led Nadeau et al. (1985) and Ahn and Peacor (1986) to propose that the uniqueness of the R1 I/S structure is related primarily to Al-Si distributions. The Al/Si ratios in the upper and lower tetrahedral sheets in one 2:1 layer are different. As a result, Al-rich (high charge) tetrahedral sheets are situated adjacent to Al-rich sheets, and Al-poor (low charge) tetrahedral sheets are adjacent to Al-poor sheets (Jiang et al. 1990a). This unique Al-Si distribution was hypothesized to cause the ordering in R1 I/S. Many data are now available implying that 1:1 R1 I/S has a unique structure and composition: (1) The composition is unique

and not a weighted average of those of smectite and illite (Jiang et al. 1990a; Jiang et al. 1992; Ransom and Helgeson 1993); (2) The occurrence of R1 I/S is apparently common relative to other mixed-layer phases, especially in that it may coexist with smectite (Ahn and Peacor 1989; Freed and Peacor 1989; Kim et al. 1995); (3) NMR data show that the Al-Si distribution in rectorite is symmetrical across the interlayer, in contrast to the distributions that are symmetrical across octahedral sheets in smectite and illite, sensu strictu (Barron et al. 1985; Altaner et al. 1988; Jakobsen et al. 1995).

This study was conducted to test the hypothesis that the unique structure of 1:1 R1 I/S should lead to unique thermodynamic properties that find expression in phase relations of the naturally occurring minerals. We infer that unique structure and thermodynamic properties should lead to common associations of the thermodynamically most stable phases. A set of samples from the Texas Gulf Coast from closely spaced depths is critical to this study because it represents the "type" and well-characterized prograde sequence; that sequence provides an apparent continuous change in I/S from smectite-rich to illite-rich (Hower et al. 1976). It allows us to trace a gradual change in the relative proportions of smectite, R1 I/S, and illite with depth. Several other samples, including a well-studied sample from Zempleni, Hungary (Srodon 1984; Reynolds 1992; Ahn and Buseck 1990; Veblen et al. 1990; Vali et al. 1994) were also included in this study. Unambiguous identification of individual smectite and illite layers is essential for estimating the relative proportions of smectite, I/S, and illite as observed in TEM images. This study has in part been made possible by development of techniques for permanent expansion of smectite-like interlayers (Kim et al. 1995). Individual smectite and illite layers can commonly be distinguished with certainty, assuring that the presence of observed relative proportions of smectite, mixed-layer I/S, and illite are truly representative of those in original rocks.

SAMPLES

Samples from five localities were used in this study. The first suite consists of a sequence of Gulf Coast samples from the Socony Mobil Oil Company No.1 Zula E. Boyd well, Dewitt County, Texas. This well penetrates a lower Miocene to Paleocene sequence of shales and sandstones to a depth of 3650 m. The main geologic unit is the Eocene Wilcox Group. Samples are mudstones or shales in the form of core cuttings from five different depths (5990'–6010', 7000'–7030', 7480'–7510', 7990'–8010', and 8990'–9010'). The shallowest unit (5990'–6010') is smectite rich and from the pre-transition zone (i.e., the shallow sequence in which the transition from smectite-rich clay to illite has not occurred). The next three samples (7000'–7030', 7480'–7510', and 7990'–8010') are from the transition zone with the upper and the lower one at the onset and end of the transition as detected by XRD data. The last sample (8990'–9010') is from the post-transition zone. Freed and Peacor (1989,

1992) determined the illite content, by XRD, of these five samples to be 20–30, 40, 50, 85, and 80%, respectively. Freed and Peacor (1992) also determined clay mineral assemblages and I/S ordering from XRD. In summary, their results show that R0 I/S is the only authigenic clay present in the samples from depths shallower than that of the smectite-to-illite transition. R1 I/S is the dominant clay in the samples from depths deeper than that of the smectite-to-illite transition. All samples have some detrital illite.

A second sample is from a closely spaced sequence from a drill core from the Nankai Trough, Japan. It is a young mudstone (<15 Ma) at a depth of 1176 m below sea floor in the form of core cuttings from the Ocean Drilling Program. It is from the post-transition zone (Masuda et al. 1995), and its illite content has been determined by XRD to be 80% (Underwood et al. 1993). Unlike the samples from the Gulf Coast in which the smectite is of detrital origin, the original smectite in Nankai Trough samples formed largely in situ by alteration of detrital volcanic glass (Masuda et al. 1996). A third sample is from Zempleni, Hungry, and was kindly provided by J. Srodon. It is illite-rich bentonite of hydrothermal origin and has been extensively studied by XRD (Srodon 1984; Reynolds 1992) and TEM (Ahn and Buseck 1990; Veblen et al. 1990; Vali et al. 1994). The fourth sample is Antrim shale from the Antrim Formation (370 Ma), Michigan Basin. It was characterized by XRD and TEM (Hover et al. 1996; Dong and Peacor 1996) and shown to have an illite content of 90%. The fifth sample is bentonite from the Welsh sedimentary basin; it is of digenetic grade and Ordovician age. XRD data showed that it contains mixed-layer I/S with 80% illite (Dong et al. 1995).

Experimental methods

XRD

Because detailed XRD results on these samples were available (Freed and Peacor 1992; Underwood et al. 1993; Srodon 1984; Hover et al. 1996; Dong and Peacor 1996), no attempt was made to characterize these samples quantitatively by XRD. X-ray diffractometer patterns were obtained before TEM observations to verify the reported relative proportions of smectite in mixed-layer I/S. XRD patterns obtained from air-dried materials were compared with those obtained from the same materials after saturation with ethylene glycol for one day.

TEM sample preparation and procedures

All samples were treated with L.R. White resin, following the procedures of Kim et al. (1995), to prevent collapse of smectite interlayers. Sticky wax-based thin sections were prepared with surfaces normal to bedding, followed by observations using back-scattered scanning electron microscopy. Typical areas that contained phyllosilicates were detached from thin sections, ion-milled, and carbon-coated for TEM observations. TEM observations were made with a Philips CM 12 scanning-trans-

mission electron microscope (STEM) fitted with a Kevex Quantum solid-state detector. The STEM was operated at 120 kV and a beam current of 20 μA. All high-resolution lattice fringe images were obtained at 100 000× magnification. The TEM magnification was originally calibrated by gold fringes and subsequently recalibrated by fringes of mineral phases with known spacings, such as muscovite. Typically, 50–60 high-quality TEM images obtained at 100 000× magnification were obtained, and mean percentages of phases (i.e., I/S, illite, etc.) were calculated from measured distributions. Identification of fringes was based on both width and contrast. Wherever possible, measurements of fringe widths were based on multiple fringes, and averages were obtained. A 20 μm objective aperture was used for imaging. Overfocus conditions (100 nm) were commonly used to optimize I/S contrast (Guthrie and Veblen 1989a, 1989b, 1990). A camera length of 770 mm and a 10 μm selected-area aperture were used to obtain SAED patterns. The camera constant calibration was performed in the same way as the TEM magnification. Quantitative EDS chemical analyses were obtained in STEM mode using a beam diameter of 5 nm and a scanning area of 30×30 nm. Standards and other conditions for chemical analyses were the same as those given by Jiang et al. (1990a).

TEM characterization of smectite, R1 I/S, and illite

All expanded samples used in this study were dominated by one or more of three specific phases: smectite, R1 I/S (50% illite), and illite. In part because many of the observations in this study are contrary to commonly accepted views, and because those results are critically dependent on the criteria used to identify phases, we first describe the collective features used to characterize each of those phases, in preparation for more detailed descriptions of the phase relations.

Smectite

Figure 1 is a TEM lattice fringe image obtained from the pre-transition sample from the Gulf Coast sequence showing typical smectite. As shown in Figure 1a, smectite displays (001) fringes having variable spacing, typically in the range 12–13 Å as opposed to the value of 10 Å, which is commonly observed for smectite in samples not treated with L.R. White resin. The variable layer spacings may be caused by structural or compositional heterogeneities (Ahn and Buseck 1990; Kim et al. 1995). The (001) fringes are anastomosing and wavy, and they change orientations by a few degrees over distances of only a few angstroms. In large part because of such changes, contrast is quite variable, even along the same fringe. There are abundant layer terminations. SAED patterns (Fig. 1b) have reflections with observable spacings only for low-order 00l reflections, with $d_{(001)} = 12$–13 Å. The 00l reflections are broad and diffuse, both parallel and normal to c^*. The streaking parallel to c^* is caused by variable spacing of 001 fringes, whereas streaking nor-
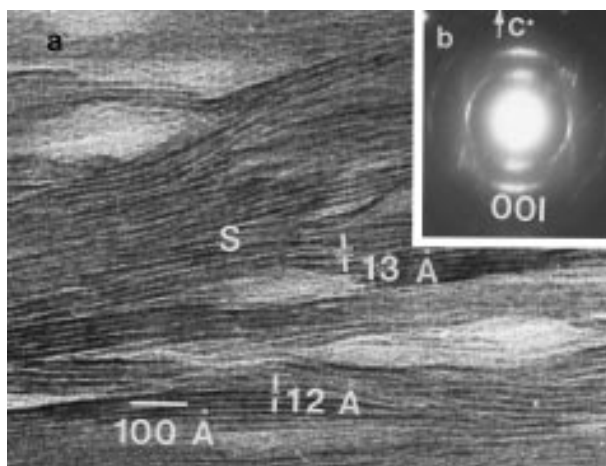
FIGURE 1. Lattice-fringe image (**a**) and corresponding SAED pattern (**b**) of smectite obtained from the pre-transition sample from the Gulf Coast sequence. (**a**) Shows 001 fringes having variable spacings, typically in the range 12–13 Å. They are anastomosing and wavy, and they change orientations by a few degrees over distances of only a few angstroms. Contrast is quite variable, even along the same fringe. (**b**) Shows the corresponding SAED patterns having reflections with observable spacings only for low-order 00*l* reflections, with $d_{(001)}$ = 12–13 Å. The 00*l* reflections are broad and diffuse, both parallel and perpendicular to *c**. Non-00*l* reflections are weak, diffuse, and nonperiodic.

TABLE 1. Typical structural formulas of smectite, R1 I/S, and illite*

	Smectite	R1 I/S	Illite
Si	7.82	6.62	6.40
[4]Al	0.18	1.38	1.60
[6]Al	2.92	3.75	3.25
Fe	0.60	0.15	0.40
Mg	0.48	0.10	0.35
Ca	0.10	0.06	0.05
Na	0.16	0.12	0.10
K	0.35	1.26	1.45

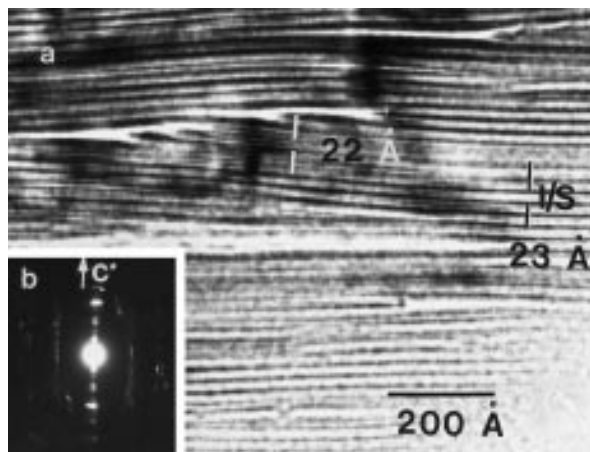 * Each formula is normalized to a total of 12 cations in tetrahedral and octahedral sites.

FIGURE 2. Lattice-fringe image (**a**) and SAED pattern (**b**) of R1 I/S obtained from illite-rich bentonite from the Welsh sedimentary basin. (**a**) Image shows 001 fringes as obtained at 100 nm overfocus condition, with alternate darker and lighter contrast having periodicity of 22–23 Å. The fringes are relatively straight compared to those of smectite, and have relatively constant spacings. The 001 layers occur as packets 7–8 layers thick. The orientations change by a few degrees over distances of tens of angstroms. Layer terminations (dislocations) are uncommon, and contrast along layers is relatively uniform. (**b**) The corresponding SAED pattern displays 00*l* reflections with $d_{(001)}$ = 22–23 Å. The 00*l* reflections are much less diffuse that those of smectite, and higher orders of 00*l* reflections can be seen. Non-00*l* reflections are somewhat ill-defined, nonperiodic, and diffuse, but less so than for smectite.

mal to *c** is caused by variable layer orientations (Dong and Peacor 1996). Non-00l reflections are weak, diffuse, and nonperiodic. AEM data (Table 1) obtained for the smectite imaged in Figure 1 give 0.3–0.4 (K + Na + Ca) per 6 cations in tetrahedral and octahedral sites, but where the dominant, and often only, detectable interlayer cation is K. These general features are consistent with the characteristics of smectite layers observed for Gulf Coast samples by Ahn and Peacor (1986), where the smectite layers had collapsed to 10 Å, and those observed by Dong and Peacor (1996) for smectite layers treated by L.R. White resin.

R1 I/S

Figure 2 is a lattice fringe image and corresponding SAED pattern obtained from illite-rich bentonite from the Welsh sedimentary basin. It shows the second type of the three distinct phases, R1 I/S (50% illite). Figure 2a was obtained at overfocus conditions and consists of (001) fringes with alternate dark and light contrast, which is consistent with images of R1 I/S (Guthrie and Veblen 1989a, 1989b, 1990). The periodicity is 22–23 Å in this case, which is compatible with lack of collapse of alternate interlayers; however, material in this sample and in all other samples usually has a slightly smaller period of 21–22 Å. The variable spacing of fringes is inferred to be due to differential expansion of the smectite-like interlayers, as caused by compositional or structural heterogenities. The fringes are relatively straight and have constant layer spacing compared to those of smectite. The

(001) layers occur as packets 7–8 layers thick. The orientations change by up to a few degrees over distances of tens of angstroms. Layer terminations (dislocations) are uncommon, and contrast along layers is relatively uniform. It must be emphasized that contrast caused by I/S ordering is not always observable, as concluded by Guthrie and Veblen (1989a, 1989b, 1990) from their computer simulation. Although most areas of Figure 2a show distinct R1 I/S contrast having periodicity of 22–23 Å, in some regions (e.g., the upper, middle part of the image) it cannot be observed. In such cases, careful measurements of spacings are needed to identify I/S ordering. Such measurements for Figure 2a show that the whole
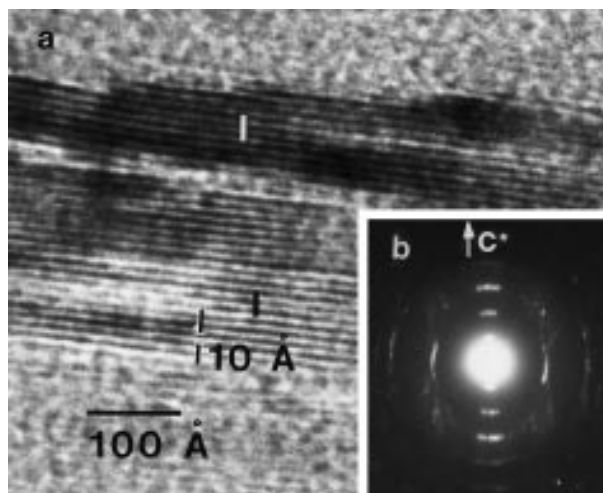
FIGURE 3. Lattice-fringe image (**a**) and corresponding SAED pattern (**b**) of illite obtained from the sample from the post-transition zone of the Gulf Coast sequence. (**a**) The image shows straight and defect-free 001 fringes, which have constant spacing of 10 Å over large distances (hundred of angstroms). Contrast is relatively uniform throughout a given packet. The 001 layers commonly occur as well-defined packets 7–8 layers thick with sharply defined boundaries on all sides, but packets commonly intersect at small angles. Layer terminations are rare. (**b**) The corresponding SAED pattern displays well-defined 00l reflections with $d_{(001)}$ = 10 Å. The diffuseness both parallel and perpendicular to c^* is much reduced relative to those for both smectite and R1 I/S.

FIGURE 4. A typical lattice-fringe image (**a**) and SAED pattern (**b**) obtained from the 5990′–6010′ depth sample of the Gulf Coast sequence. (**a**) The entire image consists of smectite only. The 001 fringes have spacings of 12–13 Å with abundant dislocations (layer terminations). The 001 layers appear to be continuous from one point to another in the image, defining a defect-rich and imperfect crystal that extends in all directions. (**b**) The SAED shows diffuse 00l reflections with periodicity of 12–13 Å and weak, diffuse, and nonperiodic non-00l reflections.

image is composed of R1 I/S. The corresponding SAED pattern (Fig. 2b) displays 00l reflections with $d_{(001)}$ = 22–23 Å. The 00l reflections are much less diffuse than those of smectite, and high orders of 00l reflections can in general be observed. Non-00l reflections are somewhat ill-defined, nonperiodic, and diffuse, but less so than for smectite. AEM data (Table 1) indicate 0.7–0.8 K (+ Na + Ca) when normalized to 6 cations in tetrahedral and octahedral sites. This composition is consistent with R1 I/S (Jiang et al. 1990a). Fringes with these features, which are collectively characteristic of R1 I/S, were commonly observed in samples from the transition zone of the Gulf Coast sequence and in those from Zempleni, the Antrim Formation, and the Nankai Trough.

Illite

Figure 3 is a lattice fringe image and corresponding SAED pattern obtained from the sample from the post-transition zone of the Gulf Coast sequence. It illustrates the third of the three distinct phases, illite. Figure 3a consists of straight and defect-free (001) fringes. The (001) layers have constant 10 Å spacing over large distances (hundreds of angstroms), indicating that these layers were not affected by L.R. White resin. Contrast is relatively uniform throughout a given packet, which is consistent with relatively constant orientation. The (001) layers commonly occur as well-defined packets with sharply de-
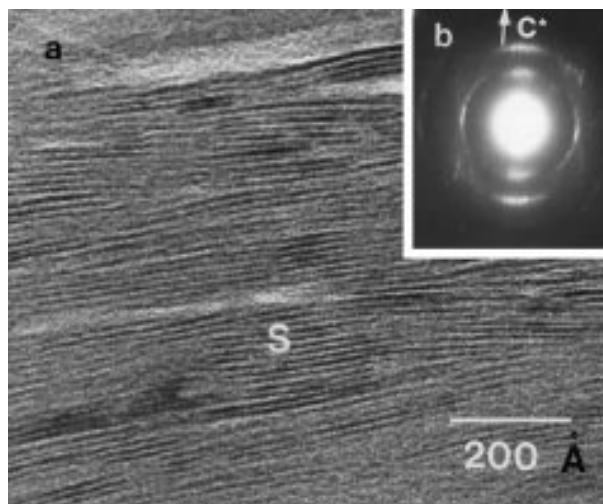
fined boundaries on all sides, but packets commonly intersect at small angles. Layer terminations are rare. The corresponding SAED pattern (Fig. 3b) shows well-defined 00l reflections with $d_{(001)}$ = 10 Å. The reduced diffuseness both parallel and normal to c^* relative to that for smectite is accounted for by the well-defined packets and constant spacing between layers. Non-00l reflections are generally nonperiodic parallel to c^*, diffuse and generally ill-defined, but less so than for R1 I/S. AEM data indicate an interlayer cation content of 0.8–0.9 K per 6 cations in tetrahedral and octahedral sites. These collective features are consistent with those of illite as described by Ahn and Peacor (1986) and Dong and Peacor (1996).

EXPERIMENTAL RESULTS

XRD data

The proportions of smectite interlayers in all samples as determined by XRD are consistent with those previously described using XRD (Freed and Peacor 1989, 1992; Underwood et al. 1993; Srodon 1984; Dong and Peacor 1996; Dong et al. 1995), verifying that the samples are representative of the desired relations.

TEM observations

5990′–6010′ depth Gulf Coast sample. Figure 4a is a typical lattice fringe image obtained for this sample. The only phyllosilicate detected within the entire image is smectite, since only fringes with 12–13 Å spacings occur with abundant dislocations (layer terminations). Although
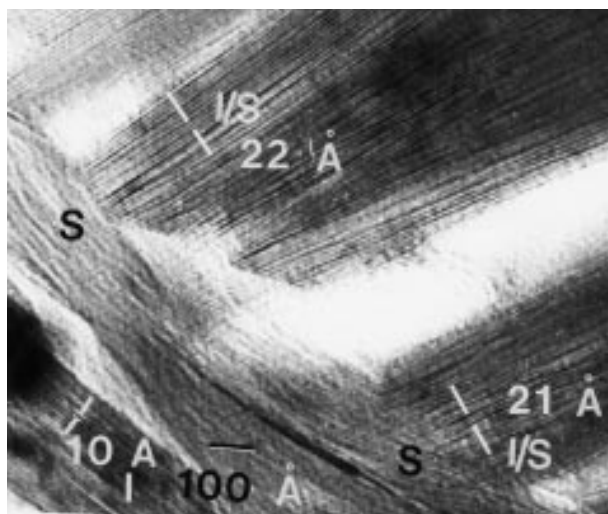
FIGURE 5. A typical lattice-fringe image for the sample from 7000′–7030′ depth of the Gulf Coast sequence. The image shows domains of three distinctly different minerals: smectite with typical 12–13 Å layer spacings (most abundant). R1 I/S with a spacing of 21–22 Å (upper and lower right corner), and illite with a spacing of 10 Å (lower left corner). The 001 fringes of R1 I/S are almost perpendicular to those of smectite, whereas the 001 fringes of illite are subparallel to those of smectite.

FIGURE 6. A typical lattice-fringe image for the sample from 7480′–7510′ depth of the Gulf Coast sequence. The image shows smectite (lower right corner), R1 I/S (upper), and illite (well-defined packet at the lower left). The low-right corner shows an along-layer boundary between smectite and illite. However, the boundaries between smectite and R1 I/S, or illite and R1 I/S, are not clearly defined.

(001) layers change orientation over a few nanometers and layers are discontinuous, one can move along and across layers in traverses where layers appear only to be coherently related. The layers thus appear to define one continuous, albeit defect-rich and imperfect, crystal that extends in all directions, forming a matrix enveloping detrital grains of minerals such as quartz. Ahn and Peacor (1986) termed such an array a "megacrystal." Figure 4b shows that the corresponding SAED pattern displays diffuse 001 reflections having periodicity of 12–13 Å and weak, diffuse, and nonperiodic non-001 reflections. Dong and Peacor (1996) showed that cross-fringes prove coherency between at least some layers over thicknesses of at least four or five layers, but with incoherency being common. The "megacrystals" can thus be viewed as highly imperfect three-dimensional crystals.

The XRD characterization of the same sample by Freed and Peacor (1992) showed that it consists of R0 I/S with 15–20% illite layers, which is qualitatively consistent with all studies of shallow, pre-transition samples from the Texas Gulf Coast. However, TEM images, of which Figure 4a is typical, were never observed to display fringes with the 10 Å spacing characteristic of an illite interlayer. On the contrary, the images always show, as in Figure 4a, interlayer spacings larger than 10 Å, which is consistent with small interlayer charges for all interlayers. Similar observations were made by Kim et al. (1995) and Dong and Peacor (1996) on smectite-rich, L.R. White resin-treated samples from the Gulf Coast. A tentative explanation is given below in the Discussion section.
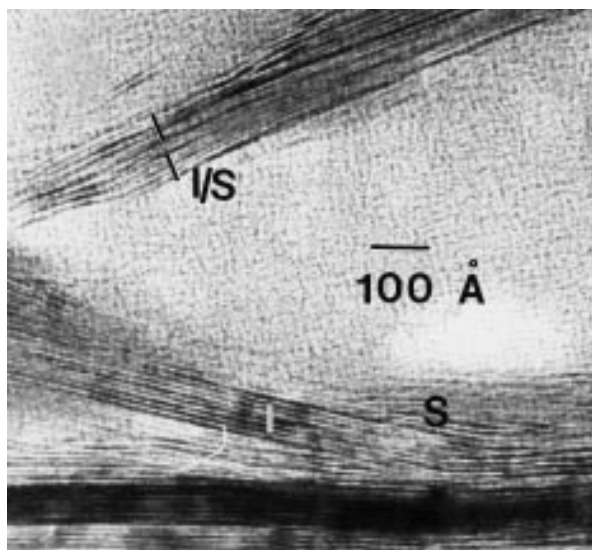
The TEM data described above show that smectite is the only dioctahedral phyllosilicate at this depth. Neither mixed-layer I/S nor authigenic illite was observed. The expanded smectite layers display features identical to those for unexpanded ones, demonstrating that the texture was not affected by L.R. White resin and that the observation of relative proportions of smectite in the ion-milled samples is representative of that in the original rocks.

7000′–7030′ depth Gulf Coast sample. According to Freed and Peacor (1989, 1992), this sample corresponds to the first stages of the smectite-to-illite transition. Figure 5 shows that it contains domains of three distinctly different minerals: (1) Smectite with typical 12–13 Å layers is most abundant. (2) R1 I/S is present with a spacing of 21–22 Å (upper portion of Fig. 5). (3) Illite with a spacing of 10 Å (lower left corner) was observed only very rarely. The ordered R1 I/S layers occur as packets within which contrast changes gradually along layers over distances of 5–10 nm. The contrast differences in alternate layers that are characteristic of R1 I/S ordering were therefore observed only locally and with difficulty.

Observation of lattice fringe images indicated that there is approximately 70–80% smectite, 20–30% R1 I/S, and only trace amounts of illite in this sample. Where there are layers having the typical alternating contrast of R1 I/S, that phase is easily identified. However, absence of that contrast may lead to misidentification of R1 I/S as smectite, based on fringe spacings greater than 10 Å, with subsequent underestimation of the proportion of R1 I/S. Therefore, the relative amount of R1 I/S detected in images of this sample is a minimum value, whereas that of smectite is a maximum.
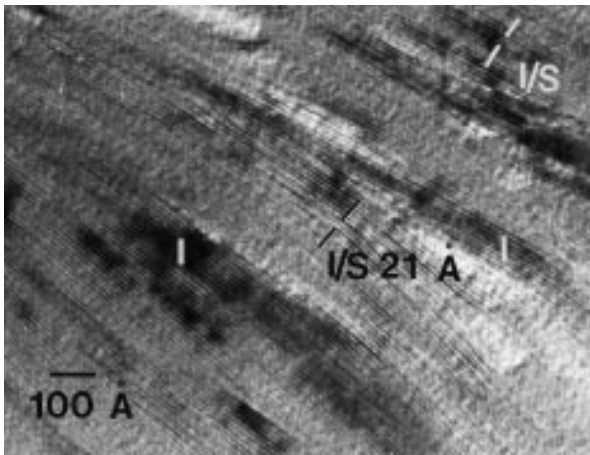
FIGURE 7. A typical lattice-fringe image for the 7990′–8010′ depth sample of the Gulf Coast sequence. It shows illite and R1 I/S only. Both illite and R1 I/S layers occur as well-defined packets with average packet thicknesses 100 Å and 70–80 Å, respectively.
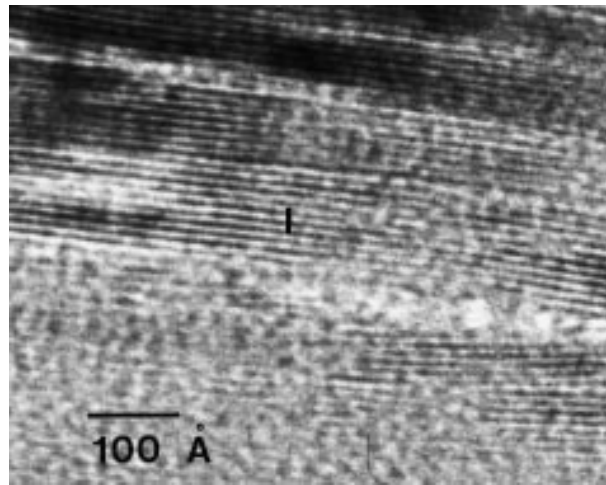

FIGURE 8. A typical lattice-fringe image for the 8990′–9010′ depth sample of the Gulf Coast sequence. The entire image consists of illite. The 001 layers have a constant spacing of 10 Å and occur as well-defined packets 8–10 layers thick.

7480′–7510′ depth Gulf Coast sample. Figure 6 is a typical TEM lattice fringe image obtained from this sample, which represents an intermediate stage of the smectite-to-illite transition. Smectite (lower right corner of the image), R1 I/S (upper part of the image), and illite (well-defined packet at the lower left) were observed as in the preceding sample but with different proportions. A well-defined along-layer boundary between smectite and illite is shown at the lower right corner of Figure 6. Approximately five layers of smectite on the right side of the boundary change to six layers of illite on the left side, implying an along-layer transition.

The relative proportions of smectite, R1 I/S, and illite are 20–30, 50–60, and 20%, respectively. Thus, there is a large decrease in the proportion of smectite and increases in those of R1 I/S and illite compared to the sample from 7000′–7030′.

7990′–8010′ depth Gulf Coast sample. As shown in Figure 7, only illite and R1 I/S were observed in this sample. Both occur as well-defined packets with average packet thicknesses of 100 Å and 70–80 Å, respectively.

The difference in appearance between illite and R1 I/S permits accurate estimates of their relative amounts. There is approximately 20–30% R1 I/S and 70–80% illite in this sample. The absence of smectite in images of this sample suggests that the smectite has completely transformed to R1 I/S and illite at this depth.

8990′–9010′ depth Gulf Coast sample. As shown in Figure 8, lattice fringes of illite dominate images of this sample. However, trace amounts of smectite were locally observed (not shown in Fig. 8). All illite layers have constant spacing of 10 Å and occur as well-defined packets 8–10 layers thick. The contrast is uniform over the whole image, suggesting constant layer orientation. The proportion of illite in this sample is > 95%.

Sample from the Nankai Trough, Japan. Figure 9 is a typical TEM image obtained from this sample, for which XRD data indicate the presence of primarily I/S. The image consists of R1 I/S (70–80%) and illite (20–30%). The R1 I/S displays typical fringe spacings of 21–22 Å with characteristic contrast. The illite layers display typical fringe spacing of 10 Å, and they occur as well-defined packets approximately 10 layers thick. Both R1 I/S and illite layers are relatively straight compared to smectite layers in the shallower samples (H. Masuda, personal communication, 1995). Individual R1 I/S and illite packets intersect one another at acute angles.
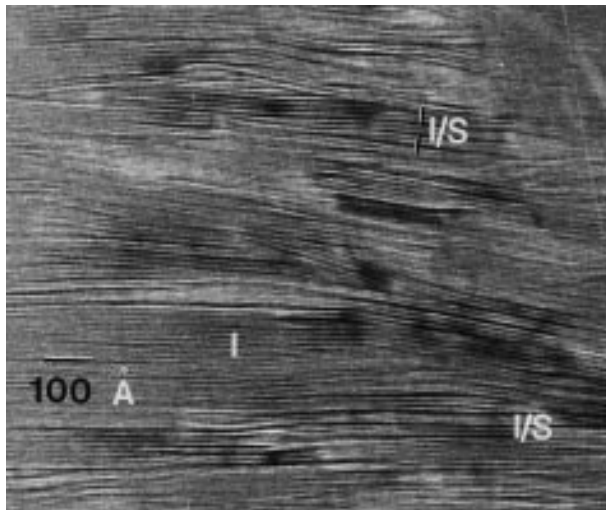

FIGURE 9. A typical lattice-fringe image for the sample from 1180 m below sea floor, Nankai Trough, Japan. The image consists of R1 I/S and illite. The R1 I/S and illite display typical fringe spacings of 21–22 Å and 10 Å, respectively. Illite layers occur as well-defined packets 10 layers thick. Individual R1 I/S and illite packets intersect one another at acute angles.
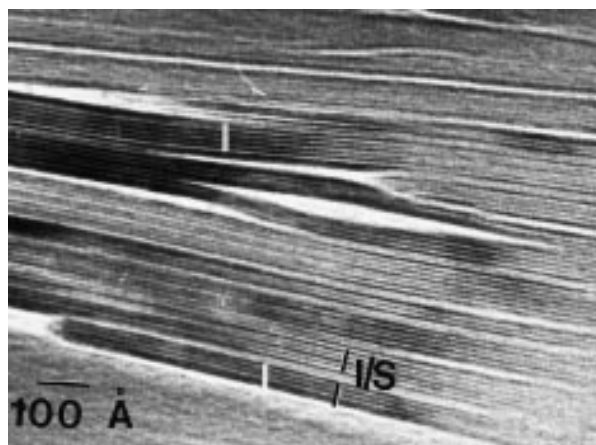
FIGURE 10. A typical lattice-fringe image for the Zempleni sample from Hungary. It shows illite having a constant spacing of 10 Å and R1 I/S having a spacing of 21–22 Å. Illite packets 40–60 Å thick are randomly mixed with R1 I/S packets 60–80 Å thick along c^*.

FIGURE 11. An example of complex layer sequences in the Zempleni sample. It shows R1, R2, R3, and R4 I/S randomly mixed in a small area of the image.

Sample from Zempleni, Hungary. Figure 10 is a typical TEM image obtained from this sample. It shows two kinds of (001) fringes. The first has constant spacing of 10 Å over large distances and is consistent with illite. The second has a 21–22 Å, spacing, which is consistent with R1 I/S. Illite packets 40–60 Å thick are randomly mixed with R1 I/S packets 60–80 Å thick along c^*. Figure 11 illustrates more complex layer relationships, showing complex sequences of layers of R1, R2, R3, and R4 I/S. However, such mixed-layer sequences were only observed locally among dozens of images. The collective images show that the sample is dominated by illite (80–90%), with R1 I/S (10%) and some R2, R3, and R4 I/S (5%). Veblen et al. (1990) and Vali et al. (1994) observed packets 3–6 layers thick (presumably R2–R5 I/S) but did not detect R1 I/S. The apparent discrepancy between previous TEM studies and this study on the same sample may be caused by experimental procedures used before TEM observations. The sample used by Veblen et al. (1990) was not treated in any way, and the one used by Vali et al. (1994) was treated with n-alkylammonium. The TEM observations of this study are also inconsistent with XRD results of Srodon (1984) on the same sample. Based on XRD results, Srodon (1984) concluded that it is comprised only of illite and R3 I/S. A tentative explanation for these differences is given below.

Sample from the Antrim Formation, Michigan Basin. Figure 12 is a representative TEM image showing two different kinds of (001) fringes. One has a 10 Å spacing as consistent with illite. The second has a 21–22 Å spacing, which is consistent with R1 I/S. R1 I/S and illite layers occur as separate, well-defined packets, intersecting at acute angles. R2 and R3 I/S were occasionally observed in this sample (e.g., see Fig. 7 of Dong and Peacor 1996). Nevertheless, illite is the dominant phase (80%), with 20% R1 I/S and minor R2 and R3 I/S.
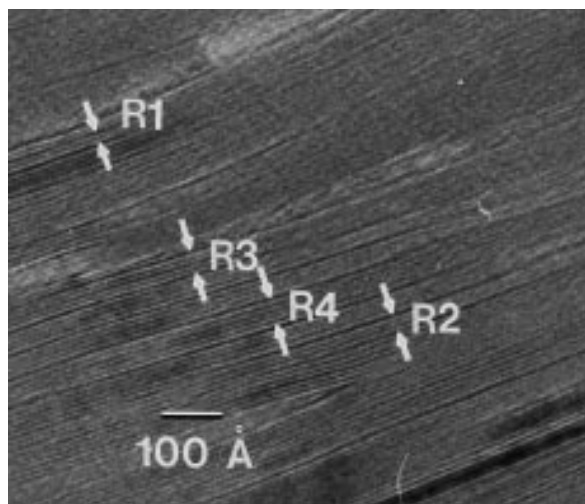
Bentonite sample from the Welsh Basin. A typical image was described in the preceding section on characterization.

DISCUSSION

Summary of results

The nine samples already described are representative of major modes of occurrence of dioctahedral phyllosilicates. These samples represent a complete prograde sequence of pelites that have undergone digenesis from the Gulf Coast, a currently transforming shale from the Nankai Trough subduction zone, a cratonic Paleozoic shale from the Antrim Formation, Michigan Basin, a hydro-

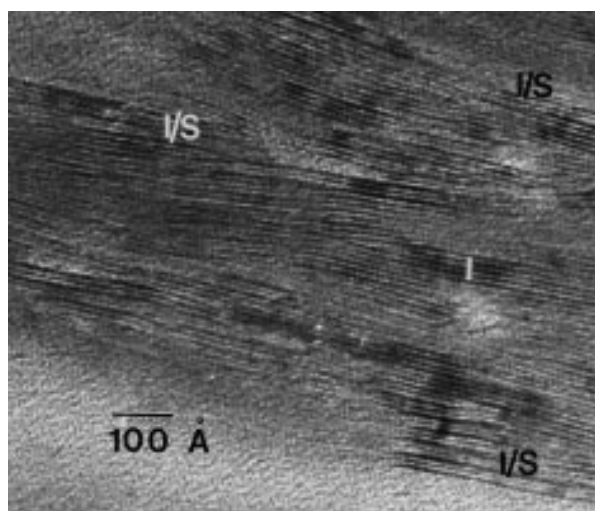**FIGURE 12.** A representative lattice-fringe image for the sample from the Michigan Basin. It shows dominant illite with a small proportion of R1 I/S. R1 I/S and illite layers occur as separate, well-defined packets, intersecting at acute angles.

thermally altered bentonite from Zempleni, and a bentonite from the Welsh sedimentary basin that was affected by regional, low-grade metamorphism. With only relatively rare exceptions, the observations demonstrate that there are three discrete phases present. They are smectite, 1:1 R1 I/S (50% illite), and illite. The observed sequence with increasing digenetic grade is (1) pure smectite, (2) smectite with small proportions of discrete R1 I/S and illite, (3) R1 I/S with small proportions of smectite and illite, (4) illite with some R1 I/S and smectite, and (5) illite. Some R2 I/S and R3 I/S were observed at stage 3 complexly interlayered with dominant R1 I/S. Even where R1 I/S is virtually the exclusive mixed-layer phase, some variation in interlayer sequence (i.e., R2 I/S, etc.) is also observed. Some smectite layers were observed at stage 4. Many variations on the simple theme presented here are possible, as emphasized below.

Comparison with a model of "continuously" variable phases

The data of this study show that R1 I/S (50% illite) is the only common mixed-layer phase in the smectite-to-illite sequence, at least in the Gulf Coast sequence and the other samples studied here. On the other hand, the XRD data of Hower et al. (1976) showed that there is a continuous change from smectite-rich clays to illite-rich clays, with the implication that such a change occurs by gradual and continuous (layer-by-layer) replacement of smectite by illite. The TEM data demonstrate, however, that the continuous aspect of such trends is due to changes in the proportions of (primarily) three discrete phases, not in proportions within single sequences of layers of individual packets.

Much controversy has surrounded the apparent differences in conclusions reached on the basis of TEM data and those of XRD data. However, we emphasize that the data are actually compatible in reflecting the same relations. The advantage of XRD is that it integrates results over discrete materials that are themselves heterogeneous in structure and composition at the atomic level, especially in that the disarticulation and reconstitution inherent in specimen preparation must result in at least limited change of structural states of clay minerals. The limited change may explain the discrepancy between XRD and TEM results for the shallow samples of the Gulf Coast sequence (i.e., the observation of R0 I/S by XRD and R1 I/S by TEM for the sample from 5990'–6010' depth). Disarticulation may preferentially occur along smectite interlayers, and reaggregation must occur randomly. However, the XRD data, when examined for compatibility with TEM data, are remarkably consistent, which they must ultimately be, since they reflect the same natural assemblages.

Phase relations among smectite, R1 I/S, and illite

The uniqueness of R1 I/S. R1 I/S is commonly viewed as consisting of alternating illite-like and smectite-like layers. However, several authors have suggested that R1 I/S does not have such a simple structure (Ahn and Peacor 1986; Jiang et al. 1990a; Vali et al. 1994; Jakobsen et al. 1995). The ordered mixed-layered structure has been hypothesized to consist of 2:1 layer units, illite-like and smectite-like, but having structures that are symmetrical across interlayers (Brown and Weir 1963; Barron et al. 1985; Ahn and Peacor 1986; Nadeau and Bain 1986; Altaner et al. 1988). Such a symmetrical relation causes the Al-Si distribution in tetrahedral sheets that are separated by interlayers to be the same. Alternate interlayers may thus be bounded by two high-charge (high Al) and two low-charge (high Si) tetrahedral sheets, respectively (Barron et al. 1985; Ahn and Peacor 1986; Altaner et al. 1988; Vali et al. 1994; Jakobsen et al. 1995). This structural state is very different from those in a sequence of separate smectite or illite 2:1 layers, wherein the Al-Si distribution must be symmetrical across the octahedral sheets, resulting in all interlayers being affected by the same interlayer charges. Symmetry across interlayers therefore provides a potential for ordering of the expandable, low-charge cation-H_2O interlayers vs. the unexpandable, high-charge, K-rich interlayers. The Al-Si distribution that is symmetrical across interlayers of R1 I/S must promote even more profound structure changes because of the atom displacements resulting from different Al-Si distributions. Additional differences must occur in the topologies of the tetrahedral sheets, which depend on the charge and ionic radii of constituent cations.

The relative positions of atoms in the 2:1 layers of ordered R1 I/S (rectorite) must be significantly different from those in either smectite or illite. Unfortunately, no direct structure refinement of rectorite has been carried out because crystals sufficiently large and well ordered for structure analysis have never been found. Layer disorder even limits structure refinement by the Rietveld method, a technique for which polycrystalline material can be used. The detailed structure topologies and charge distributions can be inferred only through indirect evidence, by analogy with ordered phases such as dolomite as described above, with TEM observations (Vali et al. 1994; Ahn and Peacor 1986; Jiang et al. 1990a), with NMR spectroscopy (Barron et al. 1985; Altaner et al. 1988; Jakobsen et al. 1995), and by chemical dissolution and cation-exchange experiments (Srodon 1980).

However, the recent conclusions of Jakobsen et al. (1995), based on NMR data, have directly corroborated Al-Si distributions that are symmetrical across interlayers. Rectorite, or 1:1 R1 I/S, is not composed of layers like those in illite and smectite. This conclusion is at the core of structural relationships and transformation mechanisms involving these minerals.

Implications for chemical composition of R1 I/S. Jiang et al. (1990a) emphasized that rectorite and other kinds of R1 I/S have a composition similar to that of illite (i.e., 0.7–0.8 K per 11 O atoms), rather than a weighted average of those of smectite and illite (e.g., 0.55 K). This relation was further developed in surveys of composition by Jiang et al. (1992) and Ransom and Helgeson (1993).

Jiang et al. (1990a) recalculated structural formulae of rectorite-like minerals published by various workers (for references, see Jiang et al. 1990a) and concluded from the calculation that the composition of rectorite is not a weighted average of equal numbers of ideal illite and smectite layers. Srodon et al. (1986, 1992) have found positive correlation between percentage of smectite-like layers in I/S samples and fixed cations, and they implied that R1 I/S has a weighted composition of smectite-like and illite-like layers. However, their compositions were based on bulk chemical analyses, and there is no direct comparison with our AEM analyses.

The fact that R1 I/S does not have a composition that a weighted average of those for smectite and illite is a direct consequence of the unique Al-Si distribution. However, because the interlayer composition must be an average of higher and lower charge values, this implies that the interlayer of lesser charge must nevertheless have charge significantly greater than that of an ideal smectite interlayer. Because only the average value is known, values for the higher and lower charge interlayers cannot be specified. However, an upper bound for the higher-charge interlayer is defined by the muscovite structure with 1.0 v.u. (defined by 1.0 K per 11 O atoms). That would require the lower charge interlayer to have a composition with approximately 0.5 v.u. However, values of 0.5 and 1.0 are limiting values for end-member phases, and intermediate phases are likely to have values such as 0.6 and 0.8 v.u.

Interlayer expansion in relation to composition. The ability of interlayers to expand upon treatment with a polar organic ion depends primarily on interlayer charge. The TEM images of samples of R1 I/S that have been expanded with L.R. White resin display R1 I/S fringes that usually have spacings of 21 Å, not a sum of layer spacings of expanded smectite (12–13 Å) and illite (10 Å), especially for the Gulf Coast sequence. There are examples where the expanded value is observed to be as large as 23 Å, but those are uncommon. The value of 21 Å is consistent with expansion of the low-charge interlayer to a value less than that observed for pure smectite. This lower expansion of R1 I/S is required by the uniqueness of the R1 structure, composition, and ordering pattern.

Ahn and Peacor (1989) emphasized that the alternating contrast typical of R1 I/S, when imaged with appropriate conditions, could be observed with ease for rectorite, but only rarely and with difficulty for R1 I/S in Gulf Coast samples. However, the spacing of R1 I/S, as well as contrast, varied from one type of sample to another. For example, TEM images of mudrock sample BRM 1311 from the Welsh sedimentary basin (Fig. 2a) display R1 I/S that has a spacing of 22–23 Å and very strong contrast, similar to that observed by Kim et al. (1995) and Ahn and Peacor (1986) for rectorite of hydrothermal origin from Arkansas. That contrast difference depends on differences in interlayer composition (Guthrie and Veblen 1989a, 1989b, 1990; Vali et al. 1994), as does expandability. We observed a general correlation between large layer spacing and strong contrast in all samples treated with L.R. White resin. That is, whenever large spacings for R1 I/S layers are observed, the TEM image also displays strong darker and lighter contrast having that periodicity. More importantly, the stronger the contrast is, the more easily and uniformly it is observed. We tentatively suggest that the relative difficulty with which contrast has been observed in lattice fringe images of Gulf Coast I/S is at least in large part simply a function of minimal difference in composition of interlayers. That is, the difference in Al/Si ratio, and therefore K content, between the upper and lower tetrahedral sheets is minimal for the Gulf Coast samples. That is consistent with an origin by transformation from smectite at <100 °C, a condition that favors disorder, in contrast with an origin for rectorite in hydrothermal veins at significantly greater temperatures.

Vali et al. (1994) showed that there is a direct relationship between expandability and the K₂O content of the samples treated with n-alkylammonium ion, and that it distinguished between different kinds of expandable material in ways that are different than for standard sample preparation for XRD, e.g., with ethylene glycol. It appears, therefore, that interlayer charge may be an important factor in distinguishing different types of R1 I/S. In this sense, ordered R1 I/S can be viewed as having heterogeneous composition and variable interlayer charge that, on average, is approximately 0.7–0.8 K per 11 O atoms, and layer periodicity of 21–23 Å for uncollapsed samples. Ideally, it should be possible to detect differences in interlayer charge by AEM and cation-exchange experiments if one particular type of R1 I/S occurs in domains large enough to characterize without any contamination from neighboring material.

Apparent incompatibilities between XRD and TEM results regarding illite percentage in mixed-layer I/S may be due to differences in expandability of interlayers as affected by the different chemicals used in specimen preparation for XRD and TEM, i.e., ethylene glycol vs. L.R. White resin. Vali et al. (1994) hypothesized such differences for n-alkylammonium treatment in contrast to ethylene glycol. That is, ethylene glycol may not be able to cause expansion of some layers for which L.R. White resin does so with ease.

In summary, the dominant dioctahedral clay minerals as observed in this study's samples are smectite, R1 I/S, and illite. Smectite is the dominant phase in the lowest grade, R1 I/S in middle grades, and illite at the highest grade, with various assemblages and proportions of the three phases corresponding to different grades among these three extremes. This strongly suggests that, among all possible interlayered mixtures of high- and low-charge layers, these three phases have minimum free energies.

Analogy with assemblages of carbonates. The system $CaCO_3$-$MgCO_3$ is in many ways analogous to the system smectite-illite, and because its relations are relatively familiar, it is helpful to review them here. The ideal composition of dolomite corresponds to equal proportions of

the components CaCO₃ (calcite) and MgCO₃ (magnesite). It is an ordered mixed-layer phase. However, as reviewed by Reeder (1983), the difference in radii of Mg^{2+} and Ca^{2+} results in shifts in atom positions, which cause the structure to be unique relative to a mixture of ideal calcite and magnesite components. It is not a simple mechanical mixture of layers of calcite and magnesite. A consequence is that dolomite is thermodynamically stable relative to any other ratios of $CaCO_3:MgCO_3$, and solvi exist between calcite and dolomite, and dolomite and magnesite. That is, any phase with composition between calcite and dolomite, or dolomite and magnesite, would have higher free energy than the sum of those for calcite and dolomite, or dolomite and magnesite, respectively. Calcite, dolomite (ordered calcite-magnesite), and magnesite are the only three stable phases in that system. It is important to emphasize, however, that this does not mean that phases of intermediate composition cannot occur under special conditions where they are metastable, as shown by the cases of calcian dolomite and magnesian calcite. However, such phases are relatively uncommon and occur in relatively recent rocks formed during early digenesis, tending to decompose to their more stable equivalents with time.

Analogy with assemblages of trioctahedral clay minerals. Shau et al. (1990b) summarized the mixed-layer relations involving chlorite and vermiculite or smectite layers, and they presented a model for corrensite that is similar to that hypothesized above for rectorite. In addition, Shau and Peacor (1992) documented the relations for changing proportions of smectite and chlorite layers over a prograde sequence of clay alteration in basalt, wherein the sequence extends from pure saponite to corrensite (R1 C/S) to chlorite. Inoue and Utada (1991) obtained additional XRD data implying that corrensite is a thermodynamically stable phase relative to other mixed-layer trioctahedral clays. These results collectively document the interrelations of chlorite and smectite or vermiculite layers and imply that corrensite is a unique phase. As emphasized by Shau et al. (1990a, 1990b), these interrelations, and the implications for assemblages of clay minerals, are analogous for rectorite and corrensite in dioctahedral and trioctahedral systems, respectively, based on the uniqueness of the compositions and structures.

Consequences of metastability of clay minerals. Illite, and by implication smectite and I/S, are metastable in all occurrences (Lippmann 1982; Jiang et al. 1990b; Essene and Peacor 1995) relative to assemblages containing muscovite, as shown by pelitic rocks approaching equilibrium at greenschist-facies conditions. With decreasing temperature of formation, such minerals are extremely heterogeneous with a high degree of disorder. Essene and Peacor (1995) emphasized that the occurrence of such minerals depends on kinetic factors. In a prograde sequence of volcanic glass, smectite, I/S, illite, and muscovite, the observed assemblages are determined by Ostwald step rule, i.e., they depend on the reaction paths.

The phases and assemblages observed in this study simply represent the most probable and most commonly observed relations under normal prograde conditions. However, any number of factors affecting reaction kinetics may cause other phase relations to occur. Rather than coexisting R1 I/S and illite, for example, various combinations of ordered sequences (e.g., R2 and R3 I/S) could form under some circumstances. Likewise, rather than smectite and R1 I/S, R0 smectite-rich I/S may form where, for example, kinetic factors are favorable. Furthermore, as predicted on the basis of the Ostwald step rule, the mechanism of transformation (e.g., massive vs. layer-by-layer dissolution and precipitation) from one assemblage to another must depend on kinetic factors (see below).

Smectite-to-illite transformation mechanism

The observations of this study have important implications for smectite-to-illite transformation mechanisms. Several models have been proposed, including successive replacement of smectite layers by illite layers (Hower et al. 1976) and dissolution of smectite and precipitation of illite (Ahn and Peacor 1986; Nadeau et al. 1985). For the assemblages observed in this and several other studies (e.g., Ahn and Peacor 1986, 1989; Freed and Peacor 1992; Kim et al. 1995; Dong and Peacor 1996), the sequence of continuously variable ratios of illite-like and smectite-like mixed-layer phases is not observed. R1 I/S does not have smectite-like layers, all 2:1 layers having been altered both in composition and Al-Si ordering state. The observations of this study imply a sequence of discrete steps in which assemblages of higher free energies are replaced by others with lower energies. Such changes must be by dissolution and precipitation. As emphasized by Ahn and Peacor (1986), such dissolution and precipitation may occur locally across a front advancing along a single layer or packet of layers, resulting in smectite being replaced by R1 I/S, or through massive dissolution, transport of reactants by fluids, and precipitation at distant sites as euhedral crystals in pore space. The essential aspect of all processes is dissolution and precipitation; the scale and atomic-level mechanisms may appear to be very different, however, as they depend on reaction kinetics and path.

Summarizing statements

We emphasize that smectite, R1 I/S, and illite are the three dominant phases observed within a digenetic sequence. The relations described in this paper are controversial in several ways. Much debate has surrounded aspects of the nature of naturally occurring dioctahedral clay minerals and mechanisms of transformation, focused in some cases on the apparent incompatibility of XRD and TEM data. Much of the controversy regarding the nature of mixed-layer clays and the mechanisms of transformation may well be based on attempts to force uniformity on a system for which infinite variety is possible. However, it is precisely in systems where metastable

phases exist, as in the case of most clay minerals, where the simple phase relations required by equilibrium and the phase rule are replaced by great variety and complexity as variations on a simple theme. Such variety is not only possible but to be expected. There are, however, simplifying principles, one set of which comprises the relations observed in this study, on the basis of which more complex relations may be rationalized.

REFERENCES CITED

Ahn, J.H., and Buseck, P.R. (1990) Layer-stacking sequences and structural disorder in mixed-layer illite/smectite: Image simulation and HRTEM imaging. American Mineralogist, 75, 267–275.

Ahn, J.H., and Peacor, D.R. (1986) Transmission and analytical electron microscopy of the smectite-to-illite transition. Clays and Clay Minerals, 34, 165–179.

———(1989) Illite/smectite from Gulf Coast: A reappraisal of transmission electron microscope images. Clays and Clay Minerals, 73, 542–546.

Altaner, S.P., Weiss, C.A., Jr., and Kirkpatrick, R.J. (1988) Evidence from ^{29}Si NMR for the structure of mixed-layer illite/smectite clay minerals. Nature, 331, 699–702.

Barron, P.F., Slade, P., and Frost, R.L. (1985) Ordering of aluminum in tetrahedral sites in mixed-layer 2:1 phyllosilicates by solid-state high-resolution NMR. Journal of Physical Chemistry, 89, 3880–3885.

Brown, G., and Weir, A.H. (1963) The identity of rectorite and allevardite. In Proceedings of International Clay Conference, Stockholm, Sweden, 27–35.

Dong, H., Hall, C.M., Peacor, D.R., and Halliday, A.N. (1995) Mechanisms of argon retention in clays revealed by ^{40}Ar-^{39}Ar dating. Science, 267, 335–359.

Dong, H., and Peacor, D.R. (1996) TEM observations of coherent stacking relations in smectite, I/S and illite of shales: evidence for McEwan crystallites and dominance of 2M₁ polytypism. Clays and Clay Minerals, 44, 257–275.

Essene, E.J., and Peacor, D.R. (1995) Clay mineral thermometry–a critical review. Clays and Clay Minerals, 43, 540–553.

Freed, R.L., and Peacor, D.R. (1989) TEM lattice fringe images with R1 ordering of illite/smectite in Gulf Coast pelitic rocks (abstract) Geological Society of America Abstracts with Programs, 21, A16.

———(1992) Digenesis and the formation of authigenic illite-rich I/S crystals in Gulf Coast shales: TEM study of clay separates. Journal of Sedimentary Petrology, 62, 220–234.

Guthrie, G. D., Jr., and Veblen, D.R. (1989a) High-resolution transmission electron microscopy of mixed-layer illite/smectite: Computer simulation. Clays and Clay Minerals 37, 1–11.

———(1989b) High-resolution transmission electron microscopy applied to clay minerals. In L.M. Coyne, S.W.S. Mckeever, and D.F. Blake, Eds., Spectroscopic characterization of minerals and their surfaces. Symposia Series 415, American Chemical Society, Washington, D.C.

———(1990) Interpreting one-dimensional high-resolution transmission electron micrographs of sheet silicates by computer simulation. American Mineralogist, 75, 276–288.

Hover, V.C., Peacor, D.R., and Walter, L.M. (1996) STEM/AEM evidence for preservation of burial digenetic fabrics in Devonian shales: Implication for fluid/rock interaction in cratonic basins (USA). Journal of Sedimentary Research, 66, 519–530.

Hower, J., Eslinger, E.V., Hower, M.E., and Perry, E.A. (1976) Mechanism of burial metamorphism of argillaceous sediments: Mineralogical and chemical evidence. Geological Society of America Bulletin, 87, 725–737.

Inoue, A., and M. Utada. (1991) Smectite-to-chlorite transformation in thermally metamorphosed volcanoclastic rocks in the Kamikita area, northern Honshu, Japan. American Mineralogist, 76, 628–640.

Jakobsen, H.J., Nielsen, N.C., and Lindgreen, H. (1995) Sequences of charged sheets in rectorite. American Mineralogist, 80, 247–252.

Jiang, W.-T., Peacor, D.R., Merriman, R.J., and Roberts, B. (1990a) Transmission and analytical electron microscopic study of mixed-layer illite-smectite formed as an apparent replacement product of digenetic illite. Clays and Clay Minerals, 38, 449–468.

Jiang, W.-T., Peacor, D.R., and Essene, E.J. (1990b) Transmission electron microscopic study of coexisting pyrophyllite and muscovite: direct evidence for the metastability of illite. Clays and Clay Minerals, 38, 225–240.

Jiang, W.-T., Fernando, N., and Peacor, D.R. (1992) Composition of digenetic illite as defined by analytical electron microscope analyses: implications for smectite-illite-muscovite transitions, Abstract 100, 29th International Geological Congress, Kyoto, Japan.

Kim, J.W., Peacor, D.R., Tessier, D., and Elsass, F. (1995) A technique for maintaining texture and permanent expansion of smectite interlayers for TEM observations. Clays and Clay Minerals, 43, 51–57.

Lippmann, F . (1982) The thermodynamic status of clay minerals. In H. van Olphen and F. Veniale, Eds., Proceedings of the International Clay Conference, Bologna, Pavia, 1981, p. 475–485. Elsevier, New York.

Masuda, H., Peacor, D.R., and Dong, H. (1995) Formation mechanisms of authigenic smectite, I/S and illite in mudstones from the Nankai Trough. In Kharaka and Chudaev, O.V., Eds., Proceedings Water-Rock Interaction-8, p. 459–462. Balkema, Rotterdam.

Masuda, H., O'Neil, J.R., Jiang, W.-T., and Peacor, D.R. (1996) Relation between interlayer composition of authigenic smectite, mineral assemblages, I/S reaction rate, and fluid composition in silicic ash of the Nankai Trough. Clays and Clay Minerals, 44, 443–459.

Nadeau, P.H., and Bain, D.C. (1986) Composition of some smectites and digenetic illitic clays and implications for their origin. Clays and Clay Minerals, 34, 455–464.

Nadeau, P.H., Wilson, M.J., Mchardy, W.J., and Tait, J.M. (1985) The conversion of smectite to illite during digenesis. Evidence from some illitic clays from bentonites and sandstones. Mineralogical Magazine, 49, 393–400.

Ransom, B., and Helgeson, H.C. (1993) Compositional end members and thermodynamic components of illite and dioctahedral aluminous smectite solid solutions. Clays and Clay Minerals, 41, 537–550.

Reeder, R.J. (1983) Crystal chemistry of the rhombohedral carbonates. In Mineralogical Society of America in Mineralogy, 11, 1–47.

Reynolds, R.C., Jr. (1988) Mixed layer chlorite minerals. In Mineralogical Society of America Reviews in Mineralogy, 19, 601–629.

———(1992) X-ray diffraction studies of illite/smectite from rocks, <1 mm randomly oriented powders and <1 mm oriented powder aggregates: The absence of laboratory-induced artifacts. Clays and Clay Minerals, 40, 387–396.

Roberson, H.E., Jenkins, D.M., and Reynolds, R.C. (1996) The 33rd Annual Meeting, The Clay Minerals Society, Program and Abstracts, 135. Gatlinburg, Tennessee.

Shau, Y.-H., Feather, M.E.M. Essene, E.J., and Peacor, D.R. (1990a) Genesis and solvus relations of submicroscopically intergrown paragonite and phengite in a blueschist from northern California. Contributions to Mineralogy and Petrology, 105, 7–72.

Shau, Y.-H., Peacor, D.R., and Essene, E.J. (1990b) Corrensite and mixed-layer chlorite/corrensite in metabasalt from northern Taiwan: TEM/AEM, EMPA, XRD and optical studies. Contribution to Mineralogy and Petrology, 105, 123–142.

Shau, Y.-H., and Peacor, D.R. (1992) Phyllosilicates in hydrothermally altered basalts from DSDP Hole 504B, Leg 83, a TEM and AEM study. Contributions to Mineralogy and Petrology, 112, 119–133.

Srodon, J. (1980) Precise identification of illite/smectite interstratifications by X-ray powder diffraction. Clays and Clay Minerals, 28, 401–411.

———(1984) X-ray powder diffraction identification of illitic materials. Clays and Clay Minerals, 32, 337–349.

Srodon, J., Morgon, D.J., Eslinger, E.V., Eberl, D.D., and Karlinger, M.R.

(1986) Chemistry of illite/smectite and end member illite. Clays and Clay Minerals, 34, 368–378.

Srodon, J., Elsass, F., McHardy, W.J., and Morgon, D.J. (1992) Chemistry of illite-smectite inferred from TEM measurements of fundamental particles. Clay Minerals, 27, 137–158.

Underwood, M., Pickering, K., Gieskes, J.M., Kastner, M., and Orr, R. (1993) Sedimentary facies evolution of the Nankai forearc and its implications for the growth of the Shimanto accretionary prism: In Hill, T.A., and Firth, J.V., Eds., Proceedings of Ocean Drilling Program, Scientific Results 131B, Ocean Drilling Program, p. 343–363. College Station, Texas.

Veblen, D.R., Guthrie, G.D., Jr., Livi, K.J.T., and Reynolds, R.C., Jr. (1990) High-resolution transmission electron microscopy and electron diffraction of mixed-layer illite/smectite: Experimental results. Clays and Clay Minerals, 38, 1–13.

Vali, H., Hesse, R., and Martin, R.F. (1994) A TEM-based definition of 2:1 layer silicates and their interstratified constituents. American Mineralogist, 79, 644–653.